CYCLIC AUTOCORRELATION, PERMUTATION FIBERS, AND A LAYERED SYMPLECTIC MODEL FOR PITCH-CLASS SPACE

JASON ST GEORGE

Abstract. We give a proof-oriented mathematical formalization of a layered musical space built from pitch-class content, cyclic order, and local permutation structure. For $G_n = \mathbb{Z}/n\mathbb{Z}$ and $1 \le k \le n$, a content set $S \subset G_n$ is encoded by its indicator function and cyclic autocorrelation, equivalently by the squared moduli of its Fourier coefficients. A rooted ordered pattern $p = (p_0, \dots, p_{k-1})$ of distinct pitch classes carries both a gap word, isolating Slonimsky-type interval-cycle structure, and an order signal, whose Fourier transform remembers the cyclic arrangement. These data define an injective layered Fourier embedding

$$\iota_{n,k} : \mathcal{P}_{n,k} \hookrightarrow \mathcal{M}_{n,k} = \mathbb{C}^{\,n-1} \times \mathbb{C}^{k}.$$

The ambient space $\mathcal{M}_{n,k}$ carries the exact symplectic form

$$\omega_{n,k}^{(\lambda)} = \frac{\mathrm{i}}{2} \sum_{j=1}^{n-1} \mathrm{d}X_j \wedge \mathrm{d}\overline{X_j} + \lambda \frac{\mathrm{i}}{2} \sum_{\ell=0}^{k-1} \mathrm{d}Y_\ell \wedge \mathrm{d}\overline{Y_\ell}, \qquad \lambda > 0,$$

which on the nonvanishing-mode locus becomes the action-angle form

$$\omega_{n,k}^{(\lambda)} = \sum_{j=1}^{n-1} \mathrm{d}I_j \wedge \mathrm{d}\theta_j + \lambda \sum_{\ell=0}^{k-1} \mathrm{d}J_\ell \wedge \mathrm{d}\phi_\ell.$$

We prove finite Wiener–Khinchin theorems for content and order, characterize periodic gap words by sparse Fourier support, construct Hamiltonian circle extensions of transposition and cyclic reindexing, show that inversion is anti-symplectic, and prove that the total space is stratified by cardinality. After reduction by transposition and finite quotient by the discrete cyclic reindexing group, one obtains symplectic orbifold strata whose singular loci are controlled by stabilizers. The result is a rigorous passage from the discrete seed of pitch-class content and order to a layered symplectic geometry suitable for exact analysis and controlled visualization.

Date: March 2026.

2020 *Mathematics Subject Classification.* Primary 53D20, 42A16; Secondary 05E18, 57S17, 00A65.

Key words and phrases. cyclic autocorrelation, discrete Fourier analysis, pitch-class sets, permutation fibers, symplectic reduction, orbifold strata, twelve-tone systems.

1. Introduction and statement of results

Let $n \geq 2$ and write $G_n = \mathbb{Z}/n\mathbb{Z}$. A nonempty subset $S \subset G_n$ records pitch-class content; an ordered k-tuple of distinct classes

$$p = (p_0, \ldots, p_{k-1}) \in \mathcal{P}_{n,k}$$

records a rooted cyclic traversal of that content. The guiding principle of this paper is that content and order must be separated before one attempts a continuous geometry. The correct exact object is not a single manifold carrying all cardinalities at once, but a family of cardinality-k strata, each of which admits a canonical spectral thickening.

The content layer is controlled by the cyclic autocorrelation of the indicator of S, following the combinatorial viewpoint of Duncan [5] and the Fourier-analytic perspective developed by Quinn [8], Amiot [9], and Yust [10]. The order layer is controlled by two signals: the gap signal, which detects periodic interval cycles in the sense suggested by Slonimsky, and the order signal, which remembers the full rooted cyclic arrangement. The resulting spectral coordinates fit naturally into the ambient complex vector space

$$\mathcal{M}_{n,k} = \mathbb{C}^{n-1} \times \mathbb{C}^k,$$

and it is this ambient space—rather than a low-dimensional picture—that carries the intrinsic geometry.

The main results are as follows.

Theorem A. For every content set $S \subset G_n$, the cyclic autocorrelation of its indicator function is the inverse Fourier transform of $|\widehat{\chi_S}|^2$. For every ordered pattern $p \in \mathcal{P}_{n,k}$, the cyclic autocorrelation of its order signal is the inverse Fourier transform of the squared moduli of its order spectrum. Consequently the content spectrum is invariant under transposition and inversion; see theorems 3.2, 3.3 and 5.3.

Theorem B. A gap word is periodic with period dividing d if and only if its gap spectrum is supported on the corresponding arithmetic progression of Fourier modes. In particular, Slonimsky-type interval cycles are exactly the minimal-period gap words, equivalently the sparsest nontrivial gap spectra; see theorems 4.1 and 4.2.

Theorem C. For every $1 \leq k \leq n$ there is an injective layered Fourier embedding

$$\iota_{n,k} : \mathcal{P}_{n,k} \hookrightarrow \mathcal{M}_{n,k} = \mathbb{C}^{n-1} \times \mathbb{C}^k$$

whose first factor records content and whose second factor records rooted cyclic order. The form

$$\omega_{n,k}^{(\lambda)} = \frac{\mathrm{i}}{2} \sum_{j=1}^{n-1} \mathrm{d}X_j \wedge \mathrm{d}\overline{X_j} + \lambda \frac{\mathrm{i}}{2} \sum_{\ell=0}^{k-1} \mathrm{d}Y_\ell \wedge \mathrm{d}\overline{Y_\ell}$$

is exact symplectic on $\mathcal{M}_{n,k}$ and becomes the full action-angle form

$$\sum_{j=1}^{n-1} \mathrm{d}I_j \wedge \mathrm{d}\theta_j + \lambda \sum_{\ell=0}^{k-1} \mathrm{d}J_\ell \wedge \mathrm{d}\phi_\ell$$

on the nonvanishing-mode locus; see theorems 6.2, 7.2 and 7.4.

Theorem D. Pitch transposition and cyclic reindexing admit commuting Hamiltonian circle extensions on $\mathcal{M}_{n,k}$ with explicit moment maps, while inversion extends to an anti-symplectic involution. The discrete musical symmetries are recovered by restricting these continuous actions to the finite subgroups coming from the roots of unity; see theorems 8.2, 8.4 and 8.6.

Theorem E. The total space

$$\mathcal{M}_n = \bigsqcup_{k=1}^{n} \mathcal{M}_{n,k}$$

is stratified by cardinality. On the open locus where the transposition action is free, Marsden–Weinstein reduction produces a symplectic manifold, and quotienting by the finite cyclic reindexing group yields a symplectic orbifold. The singular orbit-type strata are determined by explicit stabilizers, analyzed in section A; see also theorem 9.3.

The proof strategy is constructive. Sections 2–5 build the discrete seed and its Fourier invariants. Sections 6 and 7 construct the layered embedding and symplectic thickening. Sections 8 and 9 analyze the continuous symmetries, reductions, and cardinality stratification. Appendix A isolates the stabilizer calculations and the reduced-orbifold local models. Two short appendices record the exact coordinate-extraction algorithm and the role of deliberate redundancy in the layered embedding.

2. Discrete seed: content, order, and quotient actions

2.1. **Pitch classes and content.** Fix $n \geq 2$ and write $G_n = \mathbb{Z}/n\mathbb{Z}$. We denote by

$$T_t(x) = x + t, \qquad I(x) = -x, \qquad x, t \in G_n$$

the transposition and inversion actions. Together they generate the dihedral group

$$D_n = G_n \rtimes \{\pm 1\},$$

acting on G_n by affine maps $x \mapsto \pm x + t$.

Definition 2.1 (Pitch-class content)**.** A *content set* is a nonempty subset $S \subset G_n$. Its *cardinality* is $|S| = k$. The content classes modulo transposition and modulo transposition/inversion are the orbit sets

$$\mathcal{C}_n^T = (2^{G_n} \setminus \{\varnothing\})/G_n, \qquad \mathcal{C}_n^{TI} = (2^{G_n} \setminus \{\varnothing\})/D_n.$$

When $n = 12$, the orbit count is easy to compute directly by Burnside's lemma or brute force. There are 224 T/I-classes including the empty set and 223 nonempty T/I-classes.

Remark 2.2 (Forte classification and harmonic nomenclature)**.** The standard nomenclature for these classes is due to Forte [6], who assigns each T/I-class a canonical label of the form k-n, where k is the cardinality and n is the ordinal within the cardinality group. Under this system, many of the 223 classes correspond to objects familiar to every musician: 3-11 is the major/minor triad, 4-27 is the dominant/half-diminished seventh chord, 7-35 is the diatonic scale, 4-28 is the diminished seventh chord, and 6-35 is the whole-tone collection. Others—such as 5-Z12, 6-Z44, or 8-22—lack familiar common names but occupy equally definite positions in the pitch-class universe. The prefix "Z" in Forte's notation signals that a set class belongs to a homometric pair: 5-Z12 and 5-Z36, for instance, share the same interval content yet are not T/I-equivalent (see the remark on homometry in §3 below). Of the 223 classes, approximately fifty carry widely recognized names in Western music pedagogy; the remainder chart the vast majority of pitch-class space that traditional harmonic practice left unexplored.

2.2. **Ordered patterns and cyclic fibers.**

Definition 2.3 (Ordered pattern)**.** For $1 \le k \le n$, let

$$\mathcal{P}_{n,k} = \left\{ p = (p_0, \dots, p_{k-1}) \in G_n^k \,:\, p_i \neq p_j \text{ for } i \neq j \right\}$$

be the set of ordered k-tuples of distinct pitch classes. The *content projection* is

$$c : \mathcal{P}_{n,k} \to 2^{G_n}, \qquad c(p) = \{p_0, \dots, p_{k-1}\}\,.$$

Fix a content set S of size k. Then

$$\mathrm{Ord}(S) = \{p \in \mathcal{P}_{n,k} : c(p) = S\}$$

is the set of all orderings of S, hence $|\,\mathrm{Ord}(S)| = k!$.

There are two natural quotientings of order. The first is by cyclic reindexing:

$$\sigma \cdot (p_0, \dots, p_{k-1}) = (p_1, \dots, p_{k-1}, p_0),$$

which defines an action of the cyclic group C_k on $\mathrm{Ord}(S)$. The quotient $\mathrm{Ord}(S)/C_k$ records the cyclic order while forgetting the choice of starting point. The second fixes a chosen root $r \in S$ and considers only tuples with first entry r.

Definition 2.4 (Rooted cyclic fiber)**.** Let $S \subset G_n$ with $|S| = k$ and let $r \in S$. The *rooted cyclic fiber at* r is

$$\mathrm{Cyc}_r(S) = \{p \in \mathrm{Ord}(S) : p_0 = r\}\,.$$

Proposition 2.5 (Size of the rooted cyclic fiber)**.** *If $|S| = k$ and $r \in S$, then*

$$|\,\mathrm{Cyc}_r(S)| = (k-1)!.$$

Equivalently, the quotient $\mathrm{Ord}(S)/C_k$ *has* $(k-1)!$ *elements.*

Proof. Fix $p_0 = r$. The remaining $k-1$ entries may be arranged arbitrarily as a permutation of $S \setminus \{r\}$. This yields $(k-1)!$ possibilities. Since every cyclic orbit in $\mathrm{Ord}(S)$ contains exactly one representative with first entry equal to r, the same number counts $\mathrm{Ord}(S)/C_k$. □

Thus the natural *local permutation fiber* over a content point of cardinality k has size $(k-1)!$ before any further quotient by inversion or reversal.

2.3. **Gap words and reconstruction.**

Definition 2.6 (Gap word)**.** For $p = (p_0, \dots, p_{k-1}) \in \mathcal{P}_{n,k}$ define its *gap word*

$$\delta(p) = (\delta_0, \dots, \delta_{k-1}) \in G_n^k, \qquad \delta_i = p_{i+1} - p_i,$$

where indices are taken modulo k.

The gap word records the successive directed intervals of the cyclic traversal. It always satisfies

$$\sum_{i=0}^{k-1} \delta_i = 0 \quad \text{in } G_n.$$

Proposition 2.7 (Reconstruction from root and gap word)**.** *Let $r \in G_n$ and let $\delta = (\delta_0, \dots, \delta_{k-1}) \in G_n^k$. Define*

$$p_0 = r, \qquad p_m = r + \sum_{i=0}^{m-1} \delta_i \quad (1 \le m \le k-1).$$

Then $p = (p_0, \dots, p_{k-1})$ lies in $\mathcal{P}_{n,k}$ if and only if

(a) $\sum_{i=0}^{k-1} \delta_i = 0$ in G_n, and

(b) the partial sums $0, \delta_0, \delta_0 + \delta_1, \dots, \sum_{i=0}^{k-2} \delta_i$ are pairwise distinct in G_n.

In that case p is uniquely determined by (r, δ).

Proof. By construction,

$$p_{m+1} - p_m = \delta_m, \qquad 0 \le m \le k-2.$$

Moreover

$$p_0 - p_{k-1} = -\sum_{i=0}^{k-2} \delta_i = \delta_{k-1}$$

holds precisely when $\sum_i \delta_i = 0$. Distinctness of the entries is equivalent to distinctness of the partial sums. Uniqueness is immediate from the recursive formula. □

This elementary proposition is the first formal bridge between permutation space and interval cycles: the cyclic order is encoded by a constrained word in the group G_n, and Slonimsky-style cycle families appear as special periodic classes of those words.

3. Content layer: cyclic autocorrelation and spectral invariants

3.1. **Finite Fourier transform on G_n.** Let $\eta_n = e^{2\pi \mathrm{i}/n}$. For a function $f : G_n \to \mathbb{C}$, define its discrete Fourier transform by

$$\widehat{f}(j) = \sum_{x \in G_n} f(x) \eta_n^{-jx}, \qquad j \in G_n.$$

The inverse formula is

$$f(x) = \frac{1}{n} \sum_{j \in G_n} \widehat{f}(j) \eta_n^{jx}.$$

For a content set $S \subset G_n$, let χ_S be its indicator function:

$$\chi_S(x) = \begin{cases} 1, & x \in S, \\ 0, & x \notin S. \end{cases}$$

3.2. **Cyclic autocorrelation.**

Definition 3.1 (Content autocorrelation)**.** The *cyclic autocorrelation* of S is the function

$$A_S(\tau) = \sum_{x \in G_n} \chi_S(x) \chi_S(x + \tau), \qquad \tau \in G_n.$$

Thus $A_S(\tau)$ counts the number of ordered pairs $(x, y) \in S \times S$ with $y - x = \tau$. In particular $A_S(0) = |S|$ and $A_S(-\tau) = A_S(\tau)$.

Theorem 3.2 (Finite Wiener–Khinchin for content)**.** *For every content set $S \subset G_n$,*

$$\widehat{A_S}(j) = |\widehat{\chi_S}(j)|^2 \qquad (j \in G_n).$$

Equivalently,

$$A_S(\tau) = \frac{1}{n} \sum_{j \in G_n} |\widehat{\chi_S}(j)|^2 \, \eta_n^{j\tau}.$$

Proof. We compute directly:

$$\begin{aligned} \widehat{A_S}(j) &= \sum_{\tau \in G_n} A_S(\tau) \eta_n^{-j\tau} \\ &= \sum_{\tau \in G_n} \sum_{x \in G_n} \chi_S(x) \chi_S(x + \tau) \eta_n^{-j\tau}. \end{aligned}$$

Set $y = x + \tau$, so $\tau = y - x$. Then

$$\begin{aligned} \widehat{A_S}(j) &= \sum_{x, y \in G_n} \chi_S(x) \chi_S(y) \eta_n^{-j(y-x)} \\ &= \left(\sum_{y \in G_n} \chi_S(y) \eta_n^{-jy} \right) \left(\sum_{x \in G_n} \chi_S(x) \eta_n^{jx} \right) \\ &= \widehat{\chi_S}(j) \, \overline{\widehat{\chi_S}(j)} = |\widehat{\chi_S}(j)|^2 . \end{aligned}$$

The inverse formula gives the second identity. □

Corollary 3.3 (Transposition and inversion invariance)**.** *If $S' = T_t(S)$ is a transposition of S, then*

$$\widehat{\chi_{S'}}(j) = \eta_n^{-jt}\widehat{\chi_S}(j) \quad \textit{and hence} \quad A_{S'} = A_S.$$

If $S' = I(S)$ is the inversion of S, then

$$\widehat{\chi_{S'}}(j) = \widehat{\chi_S}(-j) \quad \textit{and hence} \quad A_{S'} = A_S.$$

Therefore A_S is a T/I-invariant of content.

Proof. For transposition,

$$\chi_{S'}(x) = \chi_S(x - t),$$

so

$$\widehat{\chi_{S'}}(j) = \sum_x \chi_S(x-t)\eta_n^{-jx} = \eta_n^{-jt}\sum_u \chi_S(u)\eta_n^{-ju}.$$

For inversion,

$$\chi_{S'}(x) = \chi_S(-x),$$

so

$$\widehat{\chi_{S'}}(j) = \sum_x \chi_S(-x)\eta_n^{-jx} = \sum_u \chi_S(u)\eta_n^{ju} = \widehat{\chi_S}(-j).$$

Taking moduli squared and invoking theorem 3.2 proves the claim. □

Remark 3.4 (Homometry)**.** Two content sets $S, T \subset G_n$ are homometric if $A_S = A_T$, equivalently if

$$|\widehat{\chi_S}(j)| = |\widehat{\chi_T}(j)| \qquad \text{for all } j \in G_n.$$

Thus cyclic autocorrelation is complete for interval content but not, in general, for content itself. This is exactly the finite-group form of the familiar Z-relation phenomenon in pitch-class set theory (see [6], [12]). Yust and Amiot [11] analyze the non-spectral component of transposition-invariant information, offering a complementary perspective on the information lost by the magnitude-only description.

3.3. **Moment coordinates.** The previous theorem shows that autocorrelation is a function of the nonnegative numbers

$$I_j = \frac{1}{2}\,|\widehat{\chi_S}(j)|^2\,, \qquad j = 1, \ldots, n-1.$$

These will reappear as action variables in the symplectic thickening. At this stage it is enough to note that the content autocorrelation is an affine linear image of the vector $(I_1, \ldots, I_{n-1})$, with $|S| = \widehat{\chi_S}(0)$ serving as an additional cardinality parameter.

4. Order layer I: gap words and Slonimsky spectral sparsity

4.1. **The gap signal.** The gap word records directed steps in G_n. To convert it into a Fourier-compatible signal, define

$$g_p(m) = \eta_n^{\delta_m(p)} \in S^1, \qquad m \in \mathbb{Z}/k\mathbb{Z}.$$

Its Fourier transform on $\mathbb{Z}/k\mathbb{Z}$ is

$$G_p(\ell) = \sum_{m=0}^{k-1} g_p(m)\zeta_k^{-\ell m}, \qquad \zeta_k = e^{2\pi \mathrm{i}/k}, \qquad 0 \le \ell \le k-1.$$

The signal g_p does not remember the absolute root p_0, but it encodes precisely the directed interval-cycle structure of the pattern. For the Slonimsky viewpoint this is the essential order observable.

4.2. **Periodicity versus Fourier support.** The next theorem is simply Fourier analysis on the cyclic group $\mathbb{Z}/k\mathbb{Z}$, but its music-theoretic interpretation is decisive: *periodic interval cycles are exactly the gap signals with sparse Fourier support.*

Theorem 4.1 (Periodic gap words and sparse spectra)**.** *Let d divide k and let $g : \mathbb{Z}/k\mathbb{Z} \to \mathbb{C}$. Then the following are equivalent:*

(i) $g(m+d) = g(m)$ for all m;
(ii) $\widehat{g}(\ell) = 0$ whenever ℓ is not a multiple of k/d.

Proof. Let $T_d g(m) = g(m+d)$. By a standard Fourier calculation,

$$\widehat{T_d g}(\ell) = \zeta_k^{\ell d}\widehat{g}(\ell).$$

Hence $T_d g = g$ if and only if

$$(\zeta_k^{\ell d} - 1)\widehat{g}(\ell) = 0 \qquad \text{for all } \ell.$$

Now $\zeta_k^{\ell d} = 1$ if and only if $k \mid \ell d$, equivalently if and only if ℓ is a multiple of k/d. Therefore $T_d g = g$ exactly when $\widehat{g}(\ell)$ vanishes outside those multiples. □

Corollary 4.2 (Slonimsky interval cycles)**.** *If the gap signal g_p has period d, then the order spectrum G_p is supported on the harmonic lattice*

$$\{0,\ k/d,\ 2k/d,\ \ldots,\ (d-1)k/d\} \subset \mathbb{Z}/k\mathbb{Z}.$$

In particular, principal interval cycles correspond to maximally sparse gap spectra, while interpolations and superpositions may be interpreted as controlled spectral fillings of that sparse support.

Remark 4.3. This theorem gives a rigorous mathematical language for organizing Slonimsky's families. Equal-step cycles are constant or periodic gap signals; infra-, inter-, and ultrapolations appear as perturbations of those periodic signals. In modern spectral language, the Slonimsky catalogue is arranged not only by interval arithmetic but also by the support geometry of a finite Fourier transform.

4.3. **Gap autocorrelation.** Define the gap autocorrelation by

$$B_p(r) = \sum_{m=0}^{k-1} g_p(m)\overline{g_p(m+r)}, \qquad r \in \mathbb{Z}/k\mathbb{Z}.$$

Then the same finite Wiener–Khinchin identity gives

$$\widehat{B_p}(\ell) = |G_p(\ell)|^2 .$$

Thus interval-cycle content sits in the nonnegative coordinates $|G_p(\ell)|^2$, just as pitch-class content sits in $|\widehat{\chi_S}(j)|^2$.

Remark 4.4 (Step-word entropy as a fiber invariant)**.** The gap word $\delta(p)$ induces a step histogram $h_p(s) = \#\{i : \delta_i = s\}$ on G_n. The Shannon entropy of the normalized histogram,

$$H(p) = -\sum_{s \in G_n} \frac{h_p(s)}{k} \log_2 \frac{h_p(s)}{k},$$

measures how uniformly the pattern distributes its interval steps. Orderings with a single repeated step size (equal-division cycles) have entropy zero, while orderings with maximally irregular step distributions achieve higher entropy. Within a single permutation fiber, entropy thus provides a continuous scalar invariant that distinguishes "smooth" traversals from "jagged" ones. In the companion interactive visualization, fiber vertices are colored by this entropy: low entropy appears as blue (even step spacing), high entropy as amber (irregular intervals), giving an immediate visual cue to the internal smoothness of each cyclic ordering.

5. Order layer II: faithful order signal and exact reconstruction

The gap signal is ideal for cycle periodicity, but it forgets the root. To obtain a faithful ordered encoding we use the absolute order signal.

5.1. **Order signal.**

Definition 5.1 (Order signal)**.** For $p = (p_0, \dots, p_{k-1}) \in \mathcal{P}_{n,k}$ define

$$s_p(m) = \eta_n^{p_m} \in S^1, \qquad m \in \mathbb{Z}/k\mathbb{Z}.$$

Its Fourier transform is

$$Y_p(\ell) = \sum_{m=0}^{k-1} s_p(m)\zeta_k^{-\ell m}, \qquad 0 \le \ell \le k-1.$$

The sequence s_p remembers the ordered pitch classes themselves, not only their successive differences.

Proposition 5.2 (Exact reconstruction from order Fourier data)**.** *For fixed n and k, the map*

$$p \longmapsto (Y_p(0), \dots, Y_p(k-1)) \in \mathbb{C}^k$$

is injective on $\mathcal{P}_{n,k}$.

Proof. By inverse Fourier transform on $\mathbb{Z}/k\mathbb{Z}$,

$$s_p(m) = \frac{1}{k} \sum_{\ell=0}^{k-1} Y_p(\ell) \zeta_k^{\ell m}.$$

Hence the vector $(Y_p(\ell))_{\ell=0}^{k-1}$ uniquely determines the sequence $(s_p(m))_{m=0}^{k-1}$. Each $s_p(m)$ is an nth root of unity, and therefore uniquely determines $p_m \in G_n$. Thus the whole ordered tuple p is recovered. □

5.2. **Order autocorrelation.** Define the order autocorrelation

$$C_p(r) = \sum_{m=0}^{k-1} s_p(m) \overline{s_p(m+r)}, \qquad r \in \mathbb{Z}/k\mathbb{Z}.$$

Theorem 5.3 (Finite Wiener–Khinchin for order)**.** *For every $p \in \mathcal{P}_{n,k}$,*

$$\widehat{C_p}(\ell) = |Y_p(\ell)|^2 \qquad (0 \le \ell \le k-1).$$

Proof. This is the same calculation as in theorem 3.2, applied to the function s_p on the cyclic group $\mathbb{Z}/k\mathbb{Z}$. □

Thus the order layer has its own nonnegative invariants

$$J_\ell = \frac{1}{2} |Y_p(\ell)|^2, \qquad 0 \le \ell \le k-1.$$

5.3. **Symmetries of the order signal.** Two order symmetries are particularly natural.

Proposition 5.4 (Cyclic reindexing)**.** *Let σ be the cyclic reindexing operator*

$$\sigma \cdot (p_0, \dots, p_{k-1}) = (p_1, \dots, p_{k-1}, p_0).$$

Then

$$Y_{\sigma^r p}(\ell) = \zeta_k^{\ell r} Y_p(\ell).$$

Proof. The order signal of $\sigma^r p$ is $s_p(m+r)$. Therefore

$$\begin{aligned} Y_{\sigma^r p}(\ell) &= \sum_{m=0}^{k-1} s_p(m+r) \zeta_k^{-\ell m} \\ &= \zeta_k^{\ell r} \sum_{u=0}^{k-1} s_p(u) \zeta_k^{-\ell u} = \zeta_k^{\ell r} Y_p(\ell). \end{aligned}$$

□

Proposition 5.5 (Pitch transposition and inversion)**.** *Let $T_t p = (p_0 + t, \dots, p_{k-1} + t)$ and $Ip = (-p_0, \dots, -p_{k-1})$. Then*

$$Y_{T_t p}(\ell) = \eta_n^t Y_p(\ell), \qquad Y_{Ip}(\ell) = \overline{Y_p(-\ell)}.$$

Proof. Transposition multiplies every term of s_p by η_n^t, so the same scalar factors out of the Fourier transform. Inversion sends $s_p(m)$ to $\overline{s_p(m)}$, hence

$$Y_{Ip}(\ell) = \sum_m \overline{s_p(m)}\zeta_k^{-\ell m} = \overline{\sum_m s_p(m)\zeta_k^{\ell m}} = \overline{Y_p(-\ell)}.$$

□

6. The layered Fourier embedding

We now assemble the content and order observables.

6.1. **Content coordinates.** For $p \in \mathcal{P}_{n,k}$ let $S = c(p)$ and define

$$X_p(j) = \widehat{\chi_S}(j), \qquad 1 \le j \le n-1.$$

We omit the zeroth mode because $X_p(0) = |S| = k$ is constant on the cardinality-k stratum.

6.2. **The total embedding.**

Definition 6.1 (Layered Fourier embedding)**.** For fixed (n, k) define

$$\iota_{n,k} : \mathcal{P}_{n,k} \to \mathbb{C}^{n-1} \times \mathbb{C}^k, \qquad \iota_{n,k}(p) = \big((X_p(j))_{j=1}^{n-1}, (Y_p(\ell))_{\ell=0}^{k-1}\big).$$

Proposition 6.2 (Injectivity of the layered embedding)**.** *The map $\iota_{n,k}$ is injective.*

Proof. By theorem 5.2, the order Fourier coordinates $(Y_p(\ell))_{\ell=0}^{k-1}$ alone determine p. Therefore the larger map $\iota_{n,k}$ is injective as well. □

The significance of $\iota_{n,k}$ is conceptual rather than minimal: the X-coordinates isolate content geometry, while the Y-coordinates isolate order geometry. Their coexistence makes the layered structure visible.

7. Symplectic thickening

7.1. **Ambient complex manifold.** Fix $\lambda > 0$. For each k set

$$\mathcal{M}_{n,k} = \mathbb{C}^{n-1} \times \mathbb{C}^k$$

with coordinates

$$(X_1, \dots, X_{n-1}, Y_0, \dots, Y_{k-1}).$$

Definition 7.1 (Layered symplectic form)**.** Define the 2-form

$$\omega_{n,k}^{(\lambda)} = \frac{\mathrm{i}}{2} \sum_{j=1}^{n-1} \mathrm{d}X_j \wedge \mathrm{d}\overline{X_j} + \lambda \frac{\mathrm{i}}{2} \sum_{\ell=0}^{k-1} \mathrm{d}Y_\ell \wedge \mathrm{d}\overline{Y_\ell}. \tag{7.1}$$

In real coordinates $X_j = x_j + \mathrm{i}y_j$ and $Y_\ell = u_\ell + \mathrm{i}v_\ell$,

$$\omega_{n,k}^{(\lambda)} = \sum_{j=1}^{n-1} \mathrm{d}x_j \wedge \mathrm{d}y_j + \lambda \sum_{\ell=0}^{k-1} \mathrm{d}u_\ell \wedge \mathrm{d}v_\ell.$$

Theorem 7.2 (Symplectic thickening)**.** *For every n, k and $\lambda > 0$, the pair $(\mathcal{M}_{n,k}, \omega_{n,k}^{(\lambda)})$ is an exact symplectic manifold, and*

$$\iota_{n,k}(\mathcal{P}_{n,k}) \subset \mathcal{M}_{n,k}$$

is an injective discrete subset. Hence $(\mathcal{M}_{n,k}, \omega_{n,k}^{(\lambda)})$ is a symplectic thickening of the discrete pattern space $\mathcal{P}_{n,k}$.

Proof. The form (7.1) is the direct sum of standard symplectic forms on complex vector spaces, hence closed and nondegenerate. It is exact with primitive

$$\alpha_{n,k}^{(\lambda)} = \frac{\mathrm{i}}{4} \sum_{j=1}^{n-1} \left(X_j \, \mathrm{d}\overline{X_j} - \overline{X_j} \, \mathrm{d}X_j \right) + \lambda \frac{\mathrm{i}}{4} \sum_{\ell=0}^{k-1} \left(Y_\ell \, \mathrm{d}\overline{Y_\ell} - \overline{Y_\ell} \, \mathrm{d}Y_\ell \right),$$

since $\mathrm{d}\alpha_{n,k}^{(\lambda)} = \omega_{n,k}^{(\lambda)}$. Injectivity of the discrete embedding was proved in theorem 6.2. □

Proposition 7.3 (The weight parameter is inessential)**.** *For $\lambda > 0$, the linear map*

$$F_\lambda : \mathcal{M}_{n,k} \to \mathcal{M}_{n,k}, \qquad F_\lambda(X, Y) = (X, \sqrt{\lambda}\, Y)$$

is a symplectomorphism from $(\mathcal{M}_{n,k}, \omega_{n,k}^{(1)})$ to $(\mathcal{M}_{n,k}, \omega_{n,k}^{(\lambda)})$.

Proof. A direct substitution gives

$$F_\lambda^* \omega_{n,k}^{(\lambda)} = \frac{\mathrm{i}}{2} \sum_{j=1}^{n-1} \mathrm{d}X_j \wedge \mathrm{d}\overline{X_j} + \frac{\mathrm{i}}{2} \sum_{\ell=0}^{k-1} \mathrm{d}Y_\ell \wedge \mathrm{d}\overline{Y_\ell} = \omega_{n,k}^{(1)}.$$

□

Thus λ is not an intrinsic symplectic invariant; it is a scale parameter controlling the relative size of the order fiber in renderings and numerical models.

7.2. **Action-angle coordinates.** Let

$$U_{n,k} = \{ (X, Y) \in \mathcal{M}_{n,k} : X_j \neq 0 \text{ for all } j,\ Y_\ell \neq 0 \text{ for all } \ell \}.$$

On $U_{n,k}$ write

$$X_j = \sqrt{2I_j}\, e^{\mathrm{i}\theta_j}, \qquad Y_\ell = \sqrt{2J_\ell}\, e^{\mathrm{i}\phi_\ell},$$

with $I_j, J_\ell > 0$ and $\theta_j, \phi_\ell \in \mathbb{R}/2\pi\mathbb{Z}$.

Theorem 7.4 (Full layered symplectic form)**.** *On $U_{n,k}$ one has*

$$\omega_{n,k}^{(\lambda)} = \sum_{j=1}^{n-1} \mathrm{d}I_j \wedge \mathrm{d}\theta_j + \lambda \sum_{\ell=0}^{k-1} \mathrm{d}J_\ell \wedge \mathrm{d}\phi_\ell. \tag{7.2}$$

Proof. This is the standard polar-coordinate identity

$$\frac{\mathrm{i}}{2}\,\mathrm{d}z \wedge \mathrm{d}\overline{z} = \mathrm{d}\left(\frac{1}{2}|z|^2\right) \wedge \mathrm{d}(\arg z)$$

applied to each coordinate separately and summed. □

Equation (7.2) is the *full layered symplectic form*: the content actions I_j and angles θ_j occupy the first layer, while the order actions J_ℓ and angles ϕ_ℓ occupy the second.

7.3. **Completely integrable structure.**

Theorem 7.5 (Complete integrability)**.** *On each stratum $\mathcal{M}_{n,k}$, the functions*

$$I_1, \dots, I_{n-1}, J_0, \dots, J_{k-1}$$

pairwise Poisson commute and are functionally independent on the dense open set $U_{n,k}$. Hence $(\mathcal{M}_{n,k}, \omega_{n,k}^{(\lambda)})$ is completely integrable.

Proof. In action-angle coordinates, the Poisson bracket is

$$\{F, G\} = \sum_{j=1}^{n-1}\left(\frac{\partial F}{\partial I_j}\frac{\partial G}{\partial \theta_j} - \frac{\partial F}{\partial \theta_j}\frac{\partial G}{\partial I_j}\right) + \frac{1}{\lambda}\sum_{\ell=0}^{k-1}\left(\frac{\partial F}{\partial J_\ell}\frac{\partial G}{\partial \phi_\ell} - \frac{\partial F}{\partial \phi_\ell}\frac{\partial G}{\partial J_\ell}\right).$$

Each I_j and J_ℓ depends only on itself, so all pairwise brackets vanish. Independence on $U_{n,k}$ is obvious from the coordinate system. □

Corollary 7.6 (Autocorrelation observables Poisson commute)**.** *All content autocorrelation functions $A_S(\tau)$ and all order autocorrelation functions $C_p(r)$ are functions of the commuting actions $\{I_j\}$ and $\{J_\ell\}$ respectively. Therefore any two such observables Poisson commute on the thickened space.*

Proof. By theorems 3.2 and 5.3, both families are inverse Fourier transforms of the squared Fourier moduli, hence are functions only of the actions. □

8. Hamiltonian and anti-symplectic symmetries

8.1. **Independent torus actions.** The product torus

$$\mathbb{T}^{n-1} \times \mathbb{T}^k$$

acts on $\mathcal{M}_{n,k}$ by independent phase rotations in each coordinate:

$$(a_1, \dots, a_{n-1}; b_0, \dots, b_{k-1}) \cdot (X, Y) = (a_1 X_1, \dots, a_{n-1} X_{n-1}; b_0 Y_0, \dots, b_{k-1} Y_{k-1}).$$

Its moment map is

$$\mu(X, Y) = \left(\frac{1}{2}|X_1|^2, \dots, \frac{1}{2}|X_{n-1}|^2, \frac{\lambda}{2}|Y_0|^2, \dots, \frac{\lambda}{2}|Y_{k-1}|^2\right).$$

Thus the nonnegative coordinates underlying the two autocorrelations are literally moment-map coordinates.

8.2. **Transposition.**

Definition 8.1 (Hamiltonian transposition action)**.** Define an S^1-action τ on $\mathcal{M}_{n,k}$ by

$$\tau_\alpha(X_1, \dots, X_{n-1}; Y_0, \dots, Y_{k-1}) = (e^{-\mathrm{i}\alpha} X_1, \dots, e^{-(n-1)\mathrm{i}\alpha} X_{n-1}; e^{\mathrm{i}\alpha} Y_0, \dots, e^{\mathrm{i}\alpha} Y_{k-1}), \tag{8.1}$$

where $\alpha \in \mathbb{R}/2\pi\mathbb{Z}$.

When $\alpha = 2\pi t/n$, this restricts to the discrete pitch transposition T_t on the embedded musical seed.

Theorem 8.2 (Transposition is Hamiltonian)**.** *The action τ is Hamiltonian with moment map*

$$H_T = -\sum_{j=1}^{n-1} j\, I_j + \lambda \sum_{\ell=0}^{k-1} J_\ell. \tag{8.2}$$

Proof. The infinitesimal generator of (8.1) is

$$\mathcal{X}_T = -\sum_{j=1}^{n-1} j\, \frac{\partial}{\partial \theta_j} + \sum_{\ell=0}^{k-1} \frac{\partial}{\partial \phi_\ell}.$$

Contracting with (7.2) gives

$$\iota_{\mathcal{X}_T} \omega_{n,k}^{(\lambda)} = -\sum_{j=1}^{n-1} j\, \mathrm{d}I_j + \lambda \sum_{\ell=0}^{k-1} \mathrm{d}J_\ell = \mathrm{d}H_T.$$

□

8.3. **Cyclic reindexing.**

Definition 8.3 (Hamiltonian cyclic reindexing action)**.** Define an S^1-action ρ on $\mathcal{M}_{n,k}$ by

$$\rho_\beta(X_1, \dots, X_{n-1}; Y_0, \dots, Y_{k-1}) = (X_1, \dots, X_{n-1}; e^{0\mathrm{i}\beta} Y_0, e^{1\mathrm{i}\beta} Y_1, \dots, e^{(k-1)\mathrm{i}\beta} Y_{k-1}).$$

When $\beta = 2\pi r/k$, this restricts to cyclic index shift by r on the order signal, as in theorem 5.4.

Theorem 8.4 (Cyclic reindexing is Hamiltonian)**.** *The action ρ is Hamiltonian with moment map*

$$H_R = \lambda \sum_{\ell=0}^{k-1} \ell\, J_\ell.$$

Proof. The infinitesimal generator is

$$\mathcal{X}_R = \sum_{\ell=0}^{k-1} \ell\, \frac{\partial}{\partial \phi_\ell}.$$

Thus

$$\iota_{\mathcal{X}_R} \omega_{n,k}^{(\lambda)} = \lambda \sum_{\ell=0}^{k-1} \ell\, \mathrm{d}J_\ell = \mathrm{d}H_R.$$

□

The commuting Hamiltonians H_T and H_R capture two different layers of symmetry. The action τ models pitch transposition exactly. The action ρ is a continuous Hamiltonian extension of cyclic reindexing; the actual root-forgetting operation in the discrete musical seed is recovered from the finite subgroup

$$C_k = \left\{\rho_{2\pi r/k} : 0 \le r \le k-1\right\} \subset S^1,$$

not from quotienting by the full circle. This distinction is essential in the orbifold analysis of section A.

8.4. **Inversion.**

Definition 8.5 (Inversion involution)**.** Define

$$\mathcal{I}(X_1, \dots, X_{n-1}; Y_0, \dots, Y_{k-1}) = (\overline{X_1}, \dots, \overline{X_{n-1}}; \overline{Y_0}, \overline{Y_{k-1}}, \dots, \overline{Y_1}).$$

Equivalently, in terms of order indices modulo k,

$$(\mathcal{I}Y)_\ell = \overline{Y_{-\ell}}.$$

Theorem 8.6 (Inversion is anti-symplectic)**.** *One has*

$$\mathcal{I}^2 = \mathrm{id}, \qquad \mathcal{I}^*\omega_{n,k}^{(\lambda)} = -\omega_{n,k}^{(\lambda)}.$$

Proof. Complex conjugation on each complex coordinate sends $\frac{\mathrm{i}}{2}\,\mathrm{d}z \wedge \mathrm{d}\overline{z}$ to its negative. Permutation of coordinates does not affect the form. Therefore each summand in (7.1) changes sign, and the full form does as well. □

Remark 8.7. This is the mathematically correct reason that the full T/I quotient is not globally symplectic in the naive sense: transposition is symplectic and Hamiltonian, but inversion reverses the symplectic form. The natural object is therefore a symplectic quotient by the transposition subgroup together with an anti-symplectic involution descended from inversion.

9. Reduction, fibers, and stratification

9.1. **Symplectic reduction by transposition.** By theorem 8.2, standard Marsden–Weinstein reduction applies on regular level sets of H_T (see [1, 13]). Thus, on each regular value c,

$$\mathcal{M}_{n,k} /\!\!/_c\, S^1 = H_T^{-1}(c)/S^1$$

is a symplectic orbifold of dimension

$$2(n-1+k) - 2 = 2n + 2k - 4.$$

Inside this reduced space lie the transposition classes of the embedded discrete musical patterns of cardinality k.

For the rooted order variable, the full circle action ρ supplies the Hamiltonian thickening, but the exact discrete root-forgetting operation is the finite quotient by the subgroup $C_k \subset S^1$ described above. Thus one first reduces

by transposition and then, when one wishes to forget the root of a cyclic order, passes to the finite quotient by C_k. The corresponding orbit-type strata and local orbifold charts are analyzed in section A.

9.2. **Vector-bundle interpretation.** The projection

$$\pi_{n,k} : \mathcal{M}_{n,k} \to \mathbb{C}^{n-1}, \qquad \pi_{n,k}(X, Y) = X$$

is a trivial complex vector bundle with fiber $\mathbb{C}^k$. The symplectic form splits as a product form:

$$\omega_{n,k}^{(\lambda)} = \omega_{\text{content}} \oplus \lambda\, \omega_{\text{order}}.$$

Accordingly, each cardinality-k stratum is a *content base* together with an attached *order fiber*. This is the precise mathematical version of the intuitive statement "attach each local permutation fiber to its content-class point."

Proposition 9.1 (Local permutation fibers)**.** *Fix $X \in \mathbb{C}^{n-1}$. The fiber $\pi_{n,k}^{-1}(X)$ is symplectomorphic to $(\mathbb{C}^k, \lambda\omega_{\text{std}})$. The intersection*

$$\pi_{n,k}^{-1}(X) \cap \iota_{n,k}(\mathcal{P}_{n,k})$$

is a finite set consisting of the discrete cyclic orders compatible with the content coordinates X.

Proof. The first claim is immediate from the product decomposition. For the second, $\iota_{n,k}(\mathcal{P}_{n,k})$ is discrete by construction, and fixing X fixes the content layer. What remains is a finite subset of order coordinates corresponding to the finitely many cyclic orderings of that content. □

9.3. **Stratification across cardinalities.** The full musical universe is not a single manifold because different cardinalities have different order-fiber dimensions.

Definition 9.2 (Total layered space)**.** Define

$$\mathcal{M}_n = \bigsqcup_{k=1}^{n} \mathcal{M}_{n,k}.$$

Proposition 9.3 (Stratified symplectic structure)**.** *The space $\mathcal{M}_n$ is a stratified symplectic space with strata $\mathcal{M}_{n,k}$. It is not a manifold for $n \geq 2$.*

Proof. Each $\mathcal{M}_{n,k}$ is a symplectic manifold by theorem 7.2. Their dimensions are

$$\dim \mathcal{M}_{n,k} = 2(n - 1 + k),$$

which depend on k. Since a manifold has locally constant dimension, the disjoint union cannot be a single manifold when at least two strata occur with different k. □

This proposition is the rigorous form of a point often blurred in informal geometric discussions of musical space: the global object is naturally *stratified by cardinality*. The common practice of drawing everything in one three-dimensional cloud is therefore a visualization choice, not the exact geometry.

10. Visualization theorems

The exact object lives in high-dimensional symplectic coordinates, but one may obtain faithful finite-dimensional renderings by projecting the content base and shrinking the order fibers.

10.1. **Four-dimensional direct-sum renderings.** Choose a map

$$\Phi : \mathbb{C}^{n-1} \to \mathbb{R}^2$$

representing the content base, for example by multidimensional scaling or diffusion geometry applied to a chosen content metric [14, 4]. Choose a linear or nonlinear map

$$\Psi : \mathbb{C}^k \to \mathbb{R}^2$$

representing the order fiber. For $\varepsilon > 0$ define

$$\mathcal{V}_\varepsilon^{(4)}(X, Y) = \big(\Phi(X), \varepsilon\Psi(Y)\big) \in \mathbb{R}^4.$$

This is the canonical direct-sum rendering: two coordinates for content and two for the attached order fiber. Rotating $\mathbb{R}^4$ and projecting to $\mathbb{R}^3$ or $\mathbb{R}^2$ produces the animated "4D fiber bundle" pictures used in practice.

10.2. **Three-dimensional tangent-frame renderings.** Suppose instead that the content base is embedded in $\mathbb{R}^3$ by a smooth immersion

$$\Phi : \mathcal{B} \to \mathbb{R}^3$$

defined on a content chart $\mathcal{B}$. Choose an orthonormal frame (t_1, t_2) for the normal or tangent plane used to carry the order fiber. Define

$$\mathcal{V}_\varepsilon^{(3)}(X, Y) = \Phi(X) + \varepsilon\Big(\Psi_1(Y)t_1(X) + \Psi_2(Y)t_2(X)\Big).$$

This yields the familiar "fiber discs attached to base points" picture.

Proposition 10.1 (Small-radius separation)**.** *Let $B = \{b_1, \dots, b_N\} \subset \mathbb{R}^m$ be a finite set of base points and let $F_i \subset \mathbb{R}^r$ be bounded fiber images with*

$$R = \max_i \sup_{u \in F_i} \|u\| < \infty, \qquad \delta = \min_{i \neq j} \|b_i - b_j\| > 0.$$

If $\varepsilon < \delta/(2R)$, then the translated sets

$$b_i + \varepsilon F_i$$

are pairwise disjoint.

Proof. If $u \in F_i$ and $v \in F_j$, then

$$\|(b_i + \varepsilon u) - (b_j + \varepsilon v)\| \geq \|b_i - b_j\| - \varepsilon\|u - v\| \geq \delta - 2\varepsilon R > 0.$$

Hence no two translated fiber images intersect. □

This trivial estimate is nonetheless important: it justifies the "small-radius fiber bundle" principle used in visualization. For a finite collection of content classes, one can always choose a sufficiently small fiber scale so that different fibers remain visually separated.

11. Worked consequences in the twelve-tone case

For $n = 12$, the above formalism includes, without conceptual change:

- all scale and chord contents as subsets of $\mathbb{Z}_{12}$, carrying Forte labels (e.g., 3-11 for the major/minor triad, 7-35 for the diatonic scale);
- all ordered nonrepeating patterns, including segments of twelve-tone rows;
- harmonic extensions as larger content strata containing a given subset (e.g., the dominant seventh 4-27 extends the major triad 3-11);
- Slonimsky interval cycles as periodic gap signals (e.g., equal-step cycles like the diminished seventh 4-28 and whole-tone collection 6-35);
- and local permutation fibers of size $(k-1)!$ over each content class of cardinality k.

Two numerical illustrations are shown in figures 4 and 5. They are not part of the proof theory, but they are faithful shadow projections of the exact layered architecture developed above.

Structure-aware renderings. Figure 1 shows the 223 nonempty T/I-classes of $\mathbb{Z}_{12}$ as a stratified shell graph: nodes are arranged by cardinality (radius), colored by cardinality, and sized by symmetry order; edges connect classes that differ by the addition or removal of a single pitch class. This layout makes the cardinality stratification of theorem 9.3 visually explicit and reveals the dense internal connectivity of the base quotient graph. Landmark classes are labeled by their common names ("Dim7" = Forte 4-28, "Whole-tone" = 6-35, "Octatonic" = 8-28, "Aug triad" = 3-12, "Aggregate" = 12-1).

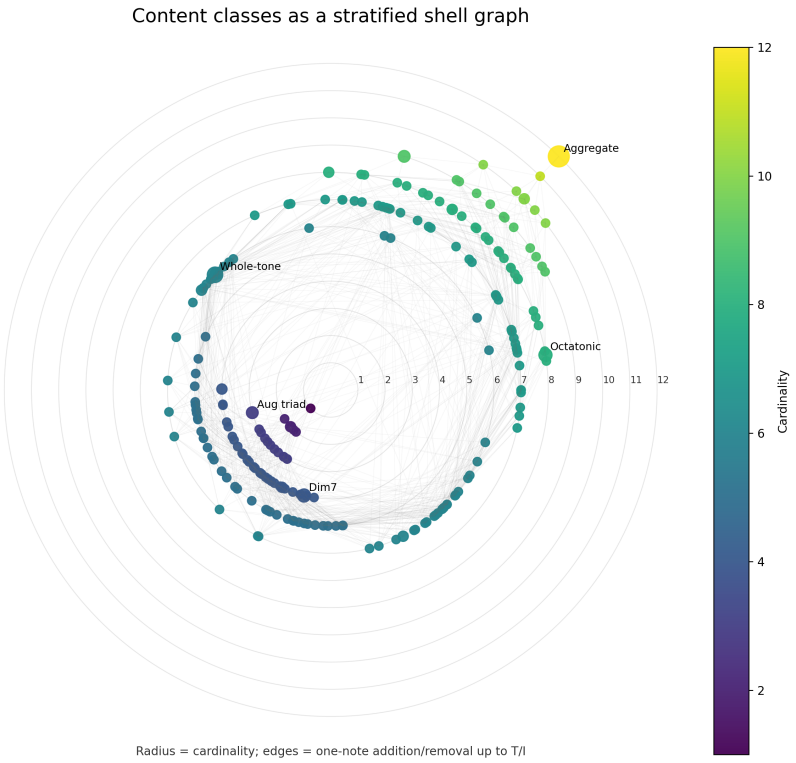

FIGURE 1. Content classes as a stratified shell graph for $n = 12$. Radius encodes cardinality; edges represent one-note addition/removal up to T/I-equivalence. Node size reflects symmetry order, making landmarks such as the whole-tone collection and diminished seventh chord visually prominent.

Attaching local permutation fibers to this shell graph yields a *rosette bundle map* in which each content node sprouts a small rosette of fiber points. Figure 2 shows this construction with fiber vertices colored by the cyclic step-word entropy $H(p)$ described in theorem 4.4. The entropy coloring exposes internal fiber structure at a glance: blue vertices correspond to smooth, evenly-spaced traversals, while yellow-green vertices indicate jagged, irregular orderings.

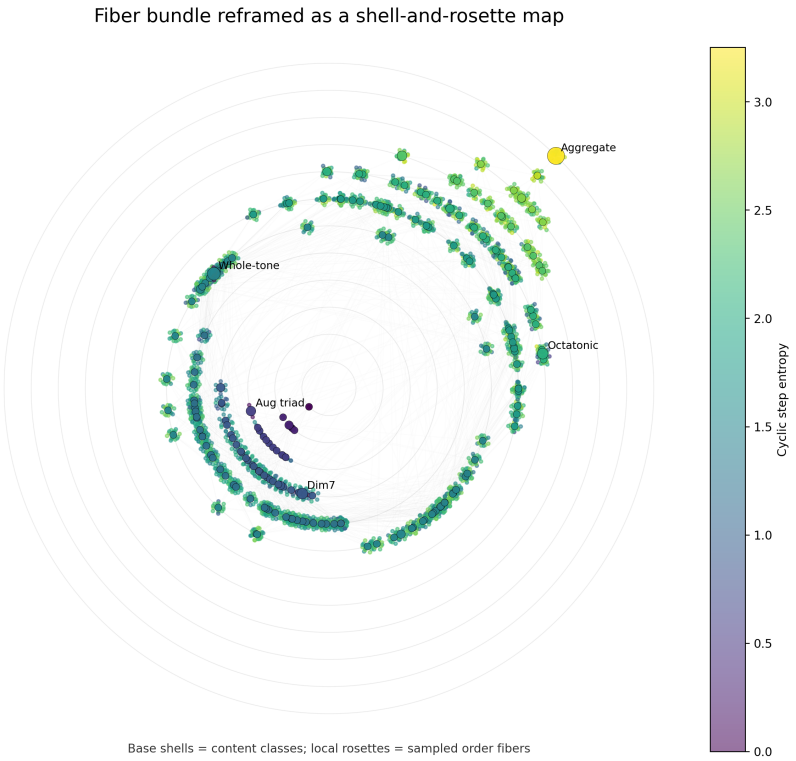

FIGURE 2. The fiber bundle reframed as a shell-and-rosette map. Base shells encode content classes; local rosettes represent sampled order fibers. Color encodes cyclic step entropy: blue indicates even step spacing (smooth traversals), yellow indicates irregular intervals (jagged orderings). This rendering is the structure-aware alternative to the generic 4D scatter figures.

Figure 3 places these structure-aware renderings alongside earlier metric-preserving prototypes.

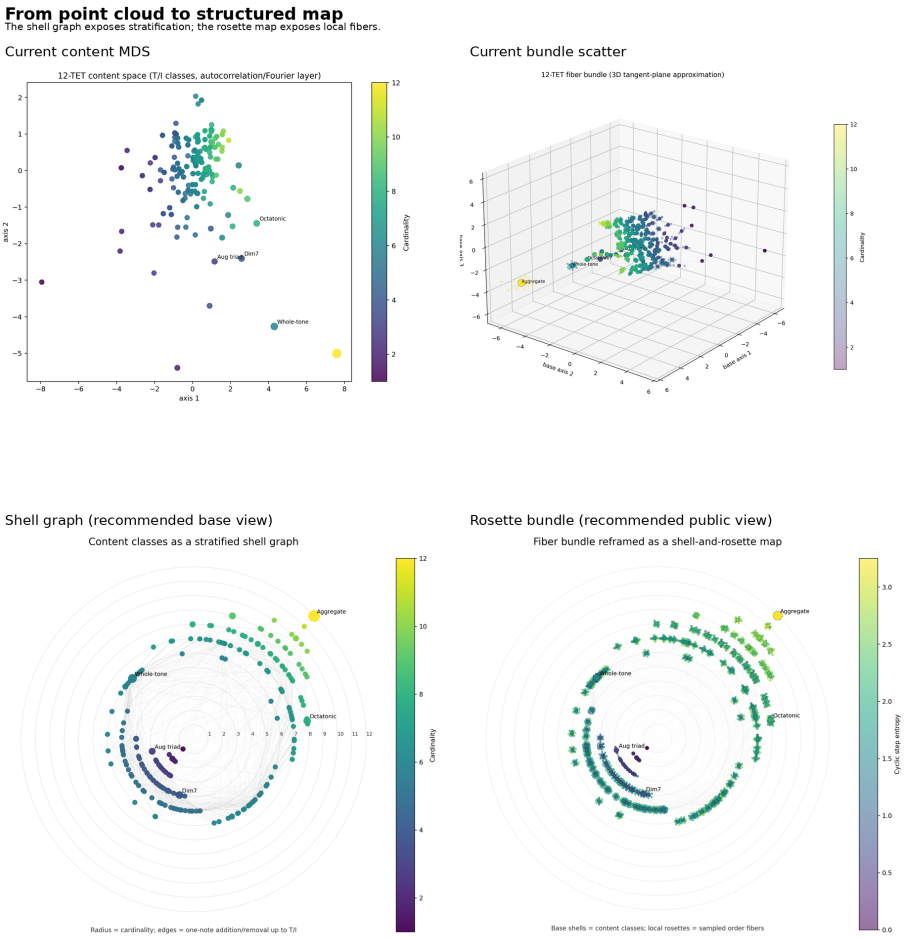

FIGURE 3. From point cloud to structured map. Top row: MDS content scatter and 3D bundle scatter from the earlier prototype. Bottom row: stratified shell graph (left) and rosette bundle map with entropy coloring (right). The shell graph exposes the cardinality stratification; the rosette map exposes local fiber structure.

Supplementary metric renderings. For completeness, figures 4 and 5 reproduce the MDS-based content scatter and 4D direct-sum projection from the earlier computational prototype. These preserve pairwise distances but do not expose the combinatorial graph skeleton; they are therefore best viewed as supplements to the shell graph and rosette map above.

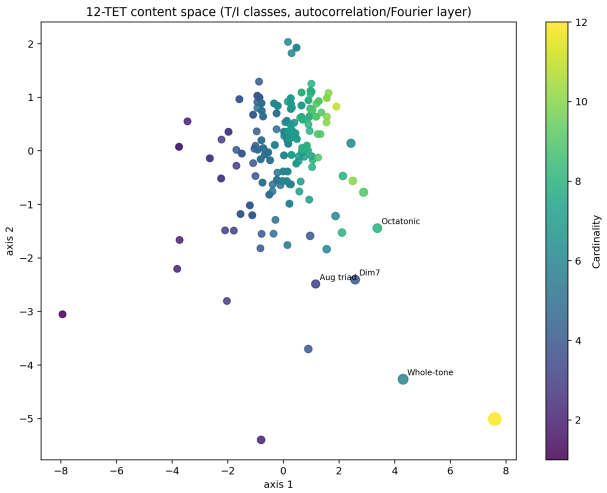

FIGURE 4. Two-dimensional content rendering via multidimensional scaling. This diagram preserves metric fidelity but does not expose the cardinality stratification visible in figure 1.

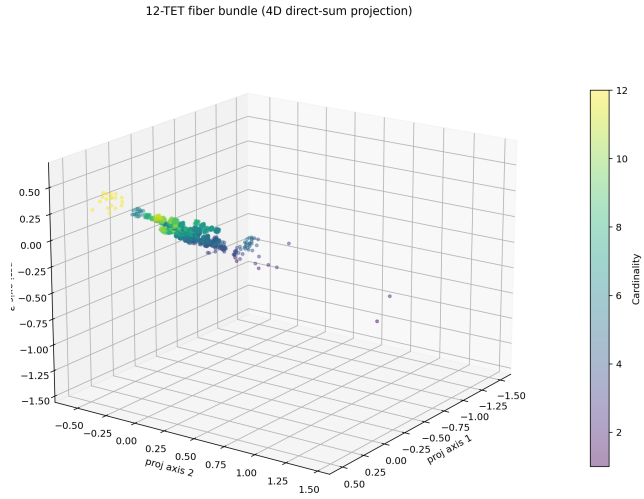

FIGURE 5. Projected 4D direct-sum rendering of the content base with attached order fibers. The exact object underlying this picture is the stratified symplectic thickening $\mathcal{M}_{12} = \bigsqcup_{k=1}^{12} \mathcal{M}_{12,k}$.

Computational anatomy of the fiber space. The fiber construction is not merely theoretical. A companion computational pipeline generates exact

or sampled fibers for every content class with three or more pitch classes (cardinalities 1 and 2 have trivial single-element fibers). Table 1 summarizes the combinatorial landscape.

TABLE 1. Fiber coverage by cardinality for the $n = 12$ case. For every content class of cardinality k, the exact count of rooted cyclic orderings is $(k-1)!$ (by theorem 2.5), independent of the symmetry order of the T/I-class. At cardinality 6 and above, the visualization samples at most 96 orderings per fiber.

Cardinality	T/I-classes	Orderings/fiber	Sampling	Total orderings
1	1	1	—	—
2	6	1	—	—
3	12	2	exhaustive	24
4	29	6	exhaustive	174
5	38	24	exhaustive	912
6	50	≤ 96	sampled from 120	4,800
7	38	≤ 96	sampled from 720	3,648
8	29	≤ 96	sampled from 5,040	2,784
9	12	≤ 96	sampled from 40,320	1,152
10	6	≤ 96	sampled from 362,880	576
11	1	≤ 96	sampled from 3,628,800	96
12	1	≤ 96	sampled from 39,916,800	96

The combinatorial explosion is dramatic: from 2 orderings at cardinality 3 to tens of millions at cardinality 12. Note that the rooted cyclic fiber count $(k-1)!$ does not depend on the symmetry order of the T/I-class: fixing a root eliminates translational symmetry. The diminished seventh chord (4-28, symmetry order 4) has the same $6 = (4-1)!$ rooted orderings as any other tetrachord. Symmetry enters only when one further quotients: the 3 distinct transpositions of the diminished seventh (versus 12 for a generic tetrachord) mean that fewer of the 6 rooted orderings give globally inequivalent patterns. Similarly, the whole-tone collection (6-35, symmetry order 6) has the full $(6-1)! = 120$ rooted orderings, but only 20 are inequivalent modulo its sixfold translational symmetry. Even the sampled fibers preserve meaningful topology, since adjacent-swap edges connect orderings differing by a single neighbor transposition, keeping the local structure of the permutohedron visible at every scale.

The full dataset contains 223 content classes, 1,051 add/remove edges, and 216 computed fibers (the seven classes of cardinality $k \leq 2$ have trivial single-element fibers and are excluded from nontrivial fiber computation) with a total of 14,166 orderings and their associated swap-edge graphs. Each content class is identified both by its Forte number and, where one exists, its common Western name (see theorem 2.2).

Worked musical case studies. We present three worked examples illustrating different corners of the framework.

Tonal: the major triad and its extensions. Let $S = \{0, 4, 7\} \subset G_{12}$ (Forte 3-11, the major/minor triad). The content spectrum is

$$X_j = 1 + \eta_{12}^{-4j} + \eta_{12}^{-7j}, \qquad 1 \le j \le 11.$$

The nonvanishing magnitudes $|X_j|$ are largest for $j = 3, 4, 5$ (the third, fourth, and fifth Fourier components), reflecting the triad's strong response to three-fold and four-fold periodicities. This spectral salience explains why the triad clusters near its harmonic extensions—4-27 (dominant seventh, $\{0, 4, 7, 10\}$), 4-26 (minor seventh, $\{0, 3, 7, 10\}$), 3-12 (augmented triad, $\{0, 4, 8\}$)—in any content rendering: their spectra share the same prominent Fourier modes.

The rooted cyclic fiber has $(3 - 1)! = 2$ orderings: $(0, 4, 7)$ and $(0, 7, 4)$, with gap words $(4, 3, 5)$ and $(7, 9, 8)$ respectively. The first is the familiar ascending arpeggiation; the second is the descending arpeggiation read as a cyclic pattern. The step-word entropy of $(4, 3, 5)$ is $H \approx 1.58$ bits (moderately irregular), while $(7, 9, 8)$ has $H \approx 1.55$ bits. Both orderings sit in the same small fiber, connected by a single adjacent swap, illustrating that at cardinality 3 the permutohedron is trivially a single edge.

Symmetry-rich: the diminished seventh chord. Let $S = \{0, 3, 6, 9\}$ (Forte 4-28, the diminished seventh chord). The stabilizer $\mathrm{Stab}_T(S) = \{0, 3, 6, 9\} \cong C_4$, so this set is invariant under transposition by any minor third. The content spectrum concentrates sharply on $j = 3$: the coefficient $|X_3|$ dominates, reflecting maximal alignment with three-fold periodicity. The remaining magnitudes $|X_j|$ vanish for $j \not\equiv 0 \pmod 3$ (apart from $j = 6, 9$), a direct consequence of the set's C_4-symmetry. Because $\mathrm{Stab}_T(S)$ has order 4, there are only $12/4 = 3$ distinct transpositions of the diminished seventh, compared with 12 for a generic tetrachord.

The rooted cyclic fiber has $(4 - 1)! = 6$ orderings. The equal-step ordering $(0, 3, 6, 9)$ has gap word $(3, 3, 3, 3)$ with entropy $H = 0$ (perfectly even). The ordering $(0, 6, 3, 9)$ has gap word $(6, 9, 6, 3)$ with entropy $H \approx 1.5$ bits. Thus the fiber displays the full range from maximally smooth to moderately jagged traversals of the same symmetric content. This example illustrates theorem 4.2: the gap word $(3, 3, 3, 3)$ is periodic with period 1, so its gap spectrum is concentrated on a single mode.

Ordered/serial: a Slonimsky-type interpolated pattern. Consider the ordered pattern $p = (0, 1, 4, 5, 8, 9)$ on the content set $S = \{0, 1, 4, 5, 8, 9\}$ (Forte 6-20). The gap word is $(1, 3, 1, 3, 1, 3)$, which is periodic with period 2: it alternates a semitone step with a minor-third leap. By theorem 4.1, the gap spectrum $G_p(\ell)$ is supported on $\{0, 3\}$ (the multiples of $k/d = 6/2 = 3$), confirming sparse spectral support. This is exactly a Slonimsky interpolation: the skeleton is a minor-third cycle $(0, 4, 8)$, and each skeleton note is followed by its chromatic upper neighbor.

The content spectrum of S has six nonvanishing modes. The dominant content mode is again $j = 3$, inherited from the minor-third backbone, but

the presence of the chromatic neighbors introduces nonzero response at other modes, distinguishing 6-20 from the bare augmented triad 3-12. In the action-angle coordinates, the content action I_3 is large while the order action J_3 dominates the order layer, so the point sits in a region of the layered space where both content and order are organized around three-fold periodicity. This spectral coherence between content and order is exactly the kind of structural alignment that the layered framework is designed to detect.

Interactive companion. An interactive realization of these renderings—the *Layered Bundle Explorer*—accompanies this paper as a web-based computational artifact. It implements all four views discussed above (MDS scatter, 4D projection, shell graph, rosette map), together with semantic zoom for progressive detail revelation, a configurable hop-radius edge filter, cardinality band selection, and on-demand fiber inspection with entropy coloring and hover tooltips. Selecting any node displays its Forte number and common name alongside its pitch-class content, fiber statistics, and step-word data. A guided-tour mode animates a traversal through musically meaningful paths—from triads through diminished ladders to whole-tone and octatonic regions—offering a narrated introduction to the bundle's topology. The explorer is available at the companion project website.

12. Conclusion

The main point of this paper is structural. The musical space generated by pitch-class content and cyclic order is not best understood as a single smooth manifold. Its correct exact form is layered and stratified:

(1) a discrete seed of content sets and rooted cyclic patterns;
(2) a content layer controlled by cyclic autocorrelation and content spectra;
(3) an interval-cycle order layer controlled by periodic gap words and their sparse spectra;
(4) a faithful order layer controlled by the Fourier transform of the order signal;
(5) a symplectic thickening on the ambient spectral coordinates;
(6) Hamiltonian circle extensions of transposition and cyclic reindexing together with a finite cyclic quotient implementing root-forgetting;
(7) and an anti-symplectic inversion symmetry yielding the final T/I-type identification.

This architecture explains several phenomena at once. Duncan's cyclic autocorrelation becomes the moment-coordinate description of pitch-class content. Slonimsky's interval cycles become periodic gap words, equivalently sparse Fourier supports. Local permutation fibers become honest vector fibers after thickening. The full continuous model carries a canonical exact symplectic form, so the geometry is not merely pictorial but Hamiltonian.

Finally, because the cardinality-k strata have dimensions $2(n-1+k)$, the total space is inherently stratified: any human-readable 3D or 4D rendering is a controlled projection of that larger exact object.

By labeling every content class with its Forte number and, where one exists, a common name from Western tonal practice, the abstract graph acquires a legible harmonic overlay. Roughly fifty of the 223 classes carry familiar names (major triad, dominant seventh, diatonic scale, whole-tone collection, and the like); the remaining majority are named only by Forte's ordinal system. This asymmetry is itself revealing: the graph topology of single-pitch-class addition/removal connects the "named" islands through long chains of "unnamed" intermediate classes, exposing the narrow scope of traditional Western harmony within the full combinatorial landscape.

Several natural extensions remain. One may add registral information and voice-leading constraints, thereby interfacing the present content/order architecture with orbifold chord spaces in the style of Tymoczko and of Callender–Quinn–Tymoczko [16, 3]. One may also replace the Euclidean content renderings by diffusion geometry or other nonlinear spectral methods [4]. But the basic formalism is already complete: from the discrete seed of pitch classes and order, one obtains a full layered symplectic form and, with it, a mathematically coherent model of the manifold intuition behind the twelve-tone universe.

Appendix A. Singular stabilizers and reduced-orbifold strata

This appendix isolates the finite stabilizers that control the singular loci of the quotient constructions. Two kinds of isotropy occur naturally: discrete stabilizers in the content quotients and finite stabilizers of the cyclic reindexing action on the thickened order fiber.

A.1. **Content stabilizers in the discrete quotient.**

Definition A.1. For a nonempty set $S \subset G_n$ define its transposition and T/I stabilizers by

$$\mathrm{Stab}_T(S) = \{t \in G_n : S + t = S\}, \qquad \mathrm{Stab}_{TI}(S) = \{g \in D_n : g(S) = S\}.$$

For $t \in G_n$ we write

$$I_t(x) = t - x$$

for the affine inversion centered at $t/2$.

Proposition A.2. *The set* $\mathrm{Stab}_T(S)$ *is a subgroup of* G_n*. Moreover* S *is a union of cosets of* $\mathrm{Stab}_T(S)$*, and conversely any subgroup* $H \leq G_n$ *with respect to which* S *is a union of cosets satisfies* $H \leq \mathrm{Stab}_T(S)$*. In particular,* $\mathrm{Stab}_T(S)$ *is nontrivial if and only if* S *is periodic under a nonzero translation.*

Proof. If $a, b \in \mathrm{Stab}_T(S)$, then

$$S + (a - b) = (S + a) - b = S - b = S,$$

so $\mathrm{Stab}_T(S)$ is a subgroup. For $s \in S$ and $h \in \mathrm{Stab}_T(S)$ one has $s + h \in S$, hence every $\mathrm{Stab}_T(S)$-coset meeting S is contained in S; therefore S is a union of such cosets. Conversely, if S is a union of cosets of a subgroup H, then $S + h = S$ for every $h \in H$, so $H \leq \mathrm{Stab}_T(S)$. The final statement is immediate. □

Proposition A.3. *Let $S \subset G_n$ be nonempty.*

(i) The affine inversion I_t stabilizes S if and only if $S = t - S$.

(ii) If no affine inversion stabilizes S, then $\mathrm{Stab}_{TI}(S) = \mathrm{Stab}_T(S)$.

(iii) If some affine inversion stabilizes S, then

$$\mathrm{Stab}_{TI}(S) = \mathrm{Stab}_T(S) \rtimes \langle I_t \rangle$$

for any such t, and in particular $|\mathrm{Stab}_{TI}(S)| = 2\,|\mathrm{Stab}_T(S)|$.

Proof. The first statement is simply the identity $I_t(S) = t - S$. For the second and third, note that every element of D_n has the form T_a or $T_a \circ I_0 = I_a$. Thus any stabilizer element with negative sign is an affine inversion preserving S. If no such inversion exists, only translations remain. Suppose now that $I_t(S) = S$. For every $h \in \mathrm{Stab}_T(S)$ one has

$$I_t \circ T_h \circ I_t = T_{-h},$$

so $\mathrm{Stab}_T(S)$ is normal in $\mathrm{Stab}_{TI}(S)$. Every sign-reversing stabilizer is of the form $T_h \circ I_t$ for some $h \in \mathrm{Stab}_T(S)$, because the product of two sign-reversing elements is a translation in $\mathrm{Stab}_T(S)$. Hence $\mathrm{Stab}_{TI}(S)$ is the claimed semidirect product and has twice the size of $\mathrm{Stab}_T(S)$. □

Remark A.4. The singular points of the finite quotient $\mathcal{C}_n^T = (2^{G_n} \setminus \{\varnothing\})/G_n$ are exactly the classes with nontrivial $\mathrm{Stab}_T(S)$, and the singular points of $\mathcal{C}_n^{TI}$ are exactly the classes with nontrivial $\mathrm{Stab}_{TI}(S)$. In the twelve-tone case, equal-step collections such as the whole-tone scale and augmented triad supply the basic examples.

A.2. **Finite stabilizers in the order fiber.** Let $C_k = \langle \rho \rangle$ be the cyclic group generated by the discrete reindexing element

$$\rho(Y_0, \ldots, Y_{k-1}) = (Y_0, \zeta_k Y_1, \ldots, \zeta_k^{k-1} Y_{k-1}), \qquad \zeta_k = e^{2\pi \mathrm{i}/k}.$$

This is the finite subgroup of the Hamiltonian circle action from theorem 8.4 corresponding to actual cyclic reindexing of rooted patterns.

Proposition A.5. *For $Y = (Y_0, \ldots, Y_{k-1}) \in \mathbb{C}^k$, let*

$$L(Y) = \{\ell \in \{0, \ldots, k-1\} : Y_\ell \neq 0\}, \qquad d(Y) = \gcd\big(\{k\} \cup L(Y)\big).$$

Then the stabilizer of Y under C_k is

$$\mathrm{Stab}_{C_k}(Y) = \left\langle \rho^{k/d(Y)} \right\rangle \cong C_{d(Y)}.$$

In particular, Y has nontrivial stabilizer if and only if every nonzero Fourier mode of Y lies in the proper subgroup $d(Y)\,\mathbb{Z}/k\mathbb{Z}$.

Proof. The condition $\rho^r Y = Y$ is equivalent to

$$e^{2\pi i r\ell/k} Y_\ell = Y_\ell$$

for every ℓ, hence to

$$k \mid r\ell \qquad \text{for all } \ell \in L(Y).$$

Write $d = d(Y)$ and $k = dk'$. Because every $\ell \in L(Y)$ is divisible by d, every multiple of k' belongs to the stabilizer: if $r = qk'$, then

$$r\ell = qk'\ell = qk\frac{\ell}{d}$$

is divisible by k. Conversely, write each $\ell \in L(Y)$ as $\ell = dm_\ell$. By definition of d, the integers k' and $\{m_\ell : \ell \in L(Y)\}$ are coprime as a family. Hence there exist integers a_ℓ and b such that

$$\sum_{\ell \in L(Y)} a_\ell m_\ell + bk' = 1.$$

If $k \mid r\ell$ for all $\ell \in L(Y)$, then $k' \mid rm_\ell$ for all such ℓ, so multiplying the Bézout identity by r shows $k' \mid r$. Therefore the stabilizer consists exactly of the classes r divisible by $k' = k/d$, which form a subgroup of order d. □

Corollary A.6. *Let $p \in \mathcal{P}_{n,k}$ and let Y be its order-spectrum coordinate in the embedding $\iota_{n,k}(p) = (X, Y)$. Then $\mathrm{Stab}_{C_k}(Y)$ is trivial.*

Proof. Assume $\mathrm{Stab}_{C_k}(Y)$ is nontrivial. By theorem A.5, there exists $d > 1$ dividing k such that $Y_\ell = 0$ whenever $d \nmid \ell$. Writing the inverse discrete Fourier transform,

$$s_p(m) = \frac{1}{k} \sum_{\ell=0}^{k-1} Y_\ell \zeta_k^{\ell m},$$

one obtains

$$s_p\left(m + \frac{k}{d}\right) = \frac{1}{k} \sum_{d \mid \ell} Y_\ell \zeta_k^{\ell m} \zeta_k^{\ell k/d} = \frac{1}{k} \sum_{d \mid \ell} Y_\ell \zeta_k^{\ell m} = s_p(m),$$

because $\zeta_k^{\ell k/d} = 1$ when $d \mid \ell$. Thus the order signal is periodic with period $k/d < k$. Since $s_p(m) = \eta_n^{p_m}$ and the map $x \mapsto \eta_n^x$ is injective on G_n, it follows that $p_{m+k/d} = p_m$ for all m, contradicting the requirement that the entries of p be distinct. □

Remark A.7. The preceding corollary shows that the embedded rooted-pattern seed lies in the regular part of the finite cyclic quotient. Singular order-fiber strata arise only after continuous thickening. By contrast, the gap signal may possess genuine periodicity on the discrete seed, and that periodicity is precisely the Slonimsky phenomenon analyzed in theorem 4.1.

A.3. **Reduced orbifold strata.** Let

$$U_{n,k} = \{(X, Y) \in \mathcal{M}_{n,k} : Y \neq 0\}$$

be the open locus on which the transposition action is free.

Lemma A.8. *The Hamiltonian transposition action τ from theorem 8.2 is free on $U_{n,k}$.*

Proof. Suppose $\tau_\alpha(X, Y) = (X, Y)$ with $Y \neq 0$. Since every order coordinate has weight 1 in equation (8.1), there exists ℓ with $Y_\ell \neq 0$, and therefore

$$e^{\mathrm{i}\alpha} Y_\ell = Y_\ell.$$

Hence $e^{\mathrm{i}\alpha} = 1$, so $\alpha = 0$ in S^1. □

For a regular value c of $H_T|_{U_{n,k}}$, define

$$Z_{n,k,c} = H_T^{-1}(c) \cap U_{n,k}, \qquad \mathcal{R}_{n,k,c} = Z_{n,k,c}/S^1.$$

Theorem A.9. *Let c be a regular value of $H_T|_{U_{n,k}}$.*

(i) $\mathcal{R}_{n,k,c}$ is a symplectic manifold.

(ii) The finite group C_k acts symplectically on $\mathcal{R}_{n,k,c}$, and the quotient

$$\mathcal{Q}_{n,k,c} = \mathcal{R}_{n,k,c}/C_k$$

is a symplectic orbifold.

(iii) For every subgroup $H \leq C_k$, the fixed-point set $\mathcal{R}^H_{n,k,c}$ is a symplectic submanifold. The orbit-type subset

$$\mathcal{R}_{n,k,c}(H) = \mathcal{R}^H_{n,k,c} \setminus \bigcup_{H \subsetneq K \leq C_k} \mathcal{R}^K_{n,k,c}$$

is open in $\mathcal{R}^H_{n,k,c}$, and its image in $\mathcal{Q}_{n,k,c}$ is an orbifold stratum with local model V/H, where V is a symplectic slice.

Proof. By theorem A.8, the S^1-action on $Z_{n,k,c}$ is free, and because c is regular, Marsden–Weinstein reduction gives a smooth symplectic manifold $\mathcal{R}_{n,k,c}$. This proves (i).

The circle actions τ and ρ commute, so the finite subgroup $C_k \subset S^1$ preserves $Z_{n,k,c}$ and descends to a symplectic action on $\mathcal{R}_{n,k,c}$. Quotients of symplectic manifolds by finite symplectic group actions are symplectic orbifolds; concretely, for $x \in \mathcal{R}_{n,k,c}$ one chooses a C_k-invariant compatible almost complex structure and metric, takes an equivariant exponential chart at x, and obtains a neighborhood modeled on a linear symplectic action of $\mathrm{Stab}_{C_k}(x)$. This proves (ii).

For (iii), fix $H \leq C_k$. Averaging any compatible almost complex structure over H yields an H-invariant compatible almost complex structure J on $\mathcal{R}_{n,k,c}$. Therefore the fixed subspace

$$(T_x \mathcal{R}_{n,k,c})^H$$

is J-invariant for every $x \in \mathcal{R}^H_{n,k,c}$, hence symplectic. Standard implicit-function arguments for finite group actions show that $\mathcal{R}^H_{n,k,c}$ is a smooth submanifold with tangent space $(T_x\mathcal{R}_{n,k,c})^H$, so it is symplectic. Because C_k is abelian, orbit types are indexed by actual subgroups rather than conjugacy classes, and $\mathcal{R}_{n,k,c}(H)$ is open in $\mathcal{R}^H_{n,k,c}$. The same equivariant chart used in (ii) gives a local quotient model V/H along this stratum. □

Corollary A.10. *The image in $\mathcal{Q}_{n,k,c}$ of every embedded rooted pattern lying in $Z_{n,k,c}$ belongs to the regular orbifold stratum.*

Proof. This is immediate from theorem A.6: the order coordinate of an embedded rooted pattern has trivial C_k-stabilizer. □

Proposition A.11. *The inversion involution $\mathcal{I}$ descends to an anti-symplectic involution*

$$\overline{\mathcal{I}} : \mathcal{Q}_{n,k,c} \to \mathcal{Q}_{n,k,c}.$$

On every smooth orbifold stratum of $\mathcal{Q}_{n,k,c}$, the fixed-point set of $\overline{\mathcal{I}}$, when nonempty, is Lagrangian.

Proof. Because $\mathcal{I}$ preserves the quantities I_j and J_ℓ, it preserves H_T and therefore $Z_{n,k,c}$. The relation

$$\mathcal{I} \circ \tau_\alpha = \tau_{-\alpha} \circ \mathcal{I}$$

shows that $\mathcal{I}$ descends through symplectic reduction to an involution of $\mathcal{R}_{n,k,c}$. Likewise

$$\mathcal{I} \circ \rho_{2\pi r/k} = \rho_{-2\pi r/k} \circ \mathcal{I},$$

so the descended involution respects the finite C_k-quotient and defines an involution $\overline{\mathcal{I}}$ on $\mathcal{Q}_{n,k,c}$. Since theorem 8.6 gives $\mathcal{I}^*\omega = -\omega$, the descended map is anti-symplectic on every orbifold chart.

Now let x lie in a smooth stratum and in the fixed-point set of $\overline{\mathcal{I}}$. In an orbifold chart V/H centered at x, choose a lift to V fixed by an anti-symplectic linear involution. The fixed subspace of an anti-symplectic linear involution is Lagrangian in V, hence its image in the local quotient is Lagrangian in the stratum. These local descriptions patch to give a Lagrangian suborbifold. □

Appendix B. Algorithmic extraction of the layered coordinates

For completeness we record the exact computational recipe for a pattern $p = (p_0, \dots, p_{k-1}) \in \mathcal{P}_{n,k}$.
Step 1: content coordinates. Set $S = \{p_0, \dots, p_{k-1}\}$ and compute

$$X_j = \sum_{x \in S} \eta_n^{-jx}, \qquad 1 \le j \le n-1.$$

Step 2: order coordinates. Compute the order signal

$$s_p(m) = \eta_n^{p_m}, \qquad 0 \le m \le k-1,$$

and then

$$Y_\ell = \sum_{m=0}^{k-1} s_p(m)\zeta_k^{-\ell m}, \qquad 0 \le \ell \le k-1.$$

Step 3: gap-spectrum coordinates (optional but musically informative). Compute the gap word

$$\delta_m = p_{m+1} - p_m \pmod{n},$$

the gap signal

$$g_p(m) = \eta_n^{\delta_m},$$

and its transform

$$G_\ell = \sum_{m=0}^{k-1} g_p(m)\zeta_k^{-\ell m}.$$

The support of G detects interval-cycle periodicity by theorem 4.1.
Step 4: symplectic coordinates. For nonzero modes write

$$X_j = \sqrt{2I_j}e^{\mathrm{i}\theta_j}, \qquad Y_\ell = \sqrt{2J_\ell}e^{\mathrm{i}\phi_\ell}.$$

Then the thickened point lies in $\mathcal{M}_{n,k}$ with symplectic form (7.2).

Appendix C. On deliberate redundancy

The order signal already determines the whole ordered pattern, whereas the content signal by itself remembers only the unordered content. Accordingly, the layered embedding is redundant. This redundancy is deliberate: it separates the two musically meaningful notions of structure. The content coordinates support content autocorrelation and transposition/inversion analysis; the order coordinates support cyclic-order analysis; and the symplectic form splits into corresponding layers. The redundancy is therefore not a defect but a categorical refinement.

References

[1] V. I. Arnold, *Mathematical Methods of Classical Mechanics*, 2nd ed., Springer, New York, 1989.

[2] L. Bigo, D. Ghisi, A. Spicher, and M. Andreatta, Representation of musical structures and processes in simplicial chord spaces, *Computer Music Journal* **39** (2015), no. 3, 9–24.

[3] C. Callender, I. Quinn, and D. Tymoczko, Generalized voice-leading spaces, *Science* **320** (2008), no. 5874, 346–348.

[4] R. R. Coifman and S. Lafon, Diffusion maps, *Applied and Computational Harmonic Analysis* **21** (2006), no. 1, 5–30.

[5] A. Duncan, Combinatorial Music Theory, *Journal of the Audio Engineering Society* **39** (1991), no. 6, 427–448.

[6] A. Forte, *The Structure of Atonal Music*, Yale University Press, New Haven, 1973.

[7] R. Morris, *Composition with Pitch-Classes: A Theory of Compositional Design*, Yale University Press, New Haven, 1987.

[8] I. Quinn, General equal-tempered harmony, *Journal of Music Theory* **50** (2006), no. 2.
[9] E. Amiot, *Music Through Fourier Space: Discrete Fourier Transform in Music Theory*, Springer, Cham, 2016.
[10] J. Yust, *Organized Time: Rhythm, Tonality, and Form*, Oxford University Press, Oxford, 2018.
[11] J. Yust and E. Amiot, Non-spectral transposition-invariant information in pitch-class sets and distributions, in *Mathematics and Computation in Music*, LNCS 13267, 279–291, 2022.
[12] J. Rahn, *Basic Atonal Theory*, Longman, New York, 1980.
[13] D. McDuff and D. Salamon, *Introduction to Symplectic Topology*, 3rd ed., Oxford University Press, Oxford, 2017.
[14] A. Samplaski, Mapping the geometries of pitch-class set similarity measures via multidimensional scaling, *Music Theory Online* **11** (2005), no. 2.
[15] N. Slonimsky, *Thesaurus of Scales and Melodic Patterns*, Scribner's, New York, 1947.
[16] D. Tymoczko, The geometry of musical chords, *Science* **313** (2006), 72–74.
[17] D. Tymoczko, *A Geometry of Music: Harmony and Counterpoint in the Extended Common Practice*, Oxford University Press, Oxford, 2011.

GAMUT (Geometric-Algebraic Music Theory) Research Program
Email address: jason@shapeofmusicalpossibility.org
URL: https://shapeofmusicalpossibility.org